EAN '97

35th International Conference on
Experimental Stress Analysis
June 4 - 6, 1997, Olomouc, Czech Republic

A NOVEL DETERMINATION OF THE COEFFICIENT OF FRICTION OF ARALDITE CT200 ON ARALDITE CT200

P Stanley and M J Johnson

Abstract

The coefficient of friction of Araldite CT200 on Araldite CT200 has been determined using a technique in which an interference-fitted disc was caused to slip on a circular shaft under the action of an applied torque. The normal contact force was determined from photoelastic observations in the fitted disc. The coefficient of friction of 0.24 was found to be independent of the normal contact force.

1. INTRODUCTION

The photoelastic stress analysis technique [1,2] is widely used for the determination of the stresses in loaded engineering components. The technique depends on the observation of the optical interference effects produced by applied loads in stress-birefringent models. The model material generally used is the cured epoxy resin Araldite CT 200 [3].

Interfacial friction is a feature of a number of stress analysis problems. A typical example is the pin-loaded lug [4,5] in which the distribution of the contact forces at the pin-lug interface is directly dependent on the frictional characteristics at the interface. It is therefore important that techniques are developed for the determination of the coefficient of friction of Araldite CT200. The paper describes the design and use of a test rig for this purpose.

2. THE TEST APPARATUS

The apparatus incorporated a CT 200 disc (outer diameter 80 mm, inner diameter 25 mm, thickness 5.0 mm) shrink-fitted onto a slightly over-size CT 200 shaft (length 125 mm, nominal diameter 5 mm). The fitting of the disc onto the shaft was effected by reducing the diameter of the shaft by cooling it in liquid nitrogen. The contact pressure at the disc-shaft interface was calculated from polariscope readings of the optical interference fringes produced in the disc as a result of the shrink-fitting. A torque loading was then applied to the disc until slip occurred. The coefficient of friction, μ, was then obtained as the ratio of the derived shear stress at the disc-shaft interface to the interfacial pressure.

A diagram of the apparatus is shown in Fig 1, in which the specimen disc is positioned at the centre of the shaft; the shaft axis was horizontal. The torque was applied to the specimen disc *via* two vertical wires attached to an annular collar fitted to the disc periphery. The applied torque was reacted by two opposite torques developed at the ends of the shaft where wires were attached to steel discs (or "pulleys") fitted to the square-sectioned ends. The three descending wires were secured into a steel plate in such a way that when the wires were taut the plate was horizontal. The ascending wires were similarly secured into a second steel

plate. The assembly was suspended from the upper plate and weights were applied to a weight-hanger attached to the centre of the lower plate. Mercer dial gauges (with 0.01 mm divisions) were used to measure the downward displacements of the shaft and the lower plate as the applied load was increased until slip occurred.

3. THEORY

3.1 Determination of contact pressure at disc-shaft interface

By combining the plane stress equilibrium equation for the case of rotational symmetry and the stress optic law equation [1] relating the isochromatic fringe order in the disc to the radial and circumferential stress difference, it can be shown that

$$\sigma_{r_i} = -p = \frac{F}{t}\int_{r_i}^{r_o}\left(\frac{n}{r}\right) dr \qquad (1)$$

where σ_{r_i} is the radial stress at the inner surface, p is the interfacial pressure, F is the material fringe value of the disc material [1], t is the disc thickness, r is the radial coordinate, and r_i and r_o are the inner and outer radii respectively. Using equation (1) p is readily determined from measured values of n at a series of r positions by graphical integration of the quantity (n/r) between r_i and r_o. (The material fringe value F was obtained from simple calibration tests on the disc material.)

Using an alternative approach based on the Lamé equations [6] it can be shown that

$$\sigma_{r_i} = -p = b(r_o^2 - r_i^2) / r_o^2 r_i^2 \qquad (2)$$

where $b/r^2 = Fn/2t$ (3)

The constant b is readily obtained from the gradient of a linear plot of n versus $1/r^2$; p then follows from equation (2).

In practice the differences in the p values obtained from equations (1) and (2) were insignificant.

3.2 Forces and displacements

A schematic diagram of the discs-shaft arrangement, with load applied, is shown in Fig 2. The symbols used are shown in the figure; the subscripts p and c denote the steel end pulleys and the collar fitted around the CT200 disc specimen respectively. It follows readily from the force and moment equilibrium requirements that

$$W_p = Wd_c / 2(d_p + d_c) \qquad \text{and} \qquad W_c = Wd_p / (d_p + d_c) \qquad (4)$$

The difference in the angular rotations θ_p and θ_c, prior to slipping, is due to the twisting of the portions of the shaft (length ℓ) between the disc specimen and the end pulleys i.e.

$$(\theta_p - \theta_c)/\ell = W_p d_p / GJ \qquad (5)$$

where G is the shear modulus of the shaft material and J is the polar second moment of area of the shaft. (Shear deformations of the end pulleys and the disc specimen are considered negligible.)

From the condition that the three upper (and lower) wires remain the same in length, using equation (5), the following equation can be derived

$$\theta_c = \left[(W_c - W_p) \frac{\ell_2}{EA} - \frac{W_p d_p^2 \ell}{2GJ} \right] \frac{2}{(d_p + d_c)} \tag{6}$$

where E and A are the Young's modulus and cross-sectional area of the supporting wires. The descent of the shaft relative to the fixed support ($\Delta\ell_1$) and the descent of the lower plate relative to the shaft ($\Delta\ell_2$) can then be evaluated from the equations

$$\Delta\ell_1 = \frac{W_c \ell_1}{EA} - \frac{d_c \theta_c}{2} \qquad \text{and} \qquad \Delta\ell_2 = \frac{W_c \ell_2}{EA} - d_c \theta_c \tag{7}$$

Although the foregoing theory (section 3.2) is not required in the interpretation of the experimental data, the outline is included for completion.

4. EXPERIMENTAL PROCEDURE AND RESULTS

There were three stages in each test:- (i) fitting the shaft into the disc, (ii) determining the isochromatic fringe distribution in the disc and (iii) the torque-slip testing.

The immersion of the shaft into the liquid nitrogen had to be done slowly in order to avoid thermal shock cracking in the CT200 material. After a soaking period in the nitrogen the shaft diameter was sufficiently reduced and the shaft could be entered and positioned in the disc without difficulty. Both shaft and disc were carefully cleaned before the fitting operation. (The maximum attainable reduction in the shaft diameter was approximately 0.25 mm.)

When the temperature of the fitted disc and shaft had returned to room temperature the isochromatic fringe order (n, see equation (1) at a series of marked radial positions along eight equi-spaced radii of the disc was determined using a diffused-light polariscope fitted with a travelling microscope. Tardy compensation [1] was used for fractional fringe order determination and care was taken to align the axis of the shaft with the axis of the polariscope. Values of the mean isochromatic fringe order at each radial position were used in determining the interfacial pressure (p, see equations (1) and (2)).

Finally the collar was fitted to the disc, the end pulleys were fitted to the shaft, wires were attached to the collar and pulleys, and the arrangement shown in Fig 1 was assembled for testing. The wire lengths were adjusted so that shaft axis and the upper and lower plates into which the wires were fitted were horizontal. The displacements of the shaft and the lower plate were recorded as the load (W, see Fig 2) was applied, initially in increments of 1 kg but in much smaller increments as the slip condition was approached. Care was taken to follow the same form of loading procedure for each test and to avoid any form of shock-loading.

The disc specimens were machined from a single plate of Araldite CT200. The material fringe value of this material (F, equation (1)), obtained from tests on a disc specimen (20 mm diameter) loaded in diametral compression, was 9.99 N/mm/fringe.

The inner diameter of each disc specimen was machined to 25.00 mm; the shaft diameters were greater than this value, the difference being the diametral interference. Five

disc-shaft assemblies were tested with nominal diametral interferences of 0.05, 0.07, 0.10 and 0.15 mm. Having taken the isochromatic fringe readings for the determination of the interfacial pressure (p), each disc-shaft assembly was loaded until slip occurred (this was indicated by a continuous increase in the displacement gauge readings with no increase in load). The value of W (see Fig 2) for which slip occurred (W^*) was noted and the corresponding value of W_c (W_c^*) was calculated from equation (4). (Note: since the diameters of the end pulleys and the collar around the disc specimens were the same (i.e. $d_p = d_c$), then $W_c^* = W^*/2$.) The coefficient of friction, μ, was then calculated from the relationship

$$\mu = W^* d_c g / \pi \, ptd^2 \qquad (8)$$

where d is the shaft diameter and g is the acceleration due to gravity. (NB. W^* is in kilograms.) Each disc-shaft assembly was tested ten times.

The results are summarised in Table 1 in which, for each assembly, the μ value obtained from the first test is given and then the average value ($\bar{\mu}$) obtained from the other nine.

Table 1 Summary of results

Specimen number	Interference (mm)	p (MPa)	μ (1st test)	($\bar{\mu}$) (average)
1	0.05	3.86	0.316	0.234
2	0.05	5.03	0.312	0.306
3	0.07	6.98	0.287	0.237
4	0.10	7.35	0.263	0.238
5	0.15	8.71	0.257	0.232

Examples of the graphs used in the determination of the integral in equation (1) and the constant b (equation (3)) are shown in Figs 3 and 4 for the 0.10 mm interference assembly. The p values obtained were 7.35 MPa and 7.36 MPa respectively. The load-displacement behaviour of a typical assembly (0.15 mm interference) can be seen in Fig 5 where sample plots of the displacement of the lower end plate ($\Delta\ell_2$, equation (9)) *versus* the applied load (W) are shown.

5. DISCUSSION

For each disc-shaft assembly tested the μ value derived from the first test was greater than those derived from the other nine tests, which generally differed by no more than a few percentage points. This effect has been attributed [7] to the microscopic asperities which are present on the original machined surface and which are removed when slip first occurs. It has been claimed [7] that molecular-level bonding can occur at these asperities. The consistency of the μ values obtained after the first test was most impressive. Except for specimen no. 1, the individual values differed from the appropriate mean value by no more than 2.6%; for specimen no. 1 the second test result of 0.216 differed from the mean (0.234) by 8%.

The $\bar{\mu}$ value obtained from specimen no. 2 was clearly not consistent with the other values. Investigation showed that this was due to a badly fitting collar assembly on the disc which had increased the contact pressure significantly above the value obtained from the photoelastic observations.

It is noteworthy that whilst the "first slip" μ value decreased with increasing interfacial

pressure, the mean of succeeding values, $\bar{\mu}$, (excluding that for the second 0.05 mm interference specimen) showed no dependence on the interfacial pressure over the range covered in the tests. The average value of $\bar{\mu}$ (excluding the 0.306 value) was 0.235.

It was observed during the development of the test method that the frictional behaviour of the disc-shaft interface may be dependent on the loading rate and that long dwell periods at loads lower than that required for slip may affect the subsequent slip load. There are clearly opportunities for further study here. The use of the technique with other material combinations might also be worthwhile.

REFERENCES

1. Durelli, A J and Riley, W F, "Introduction to Photomechanics", Prentice-Hall Inc/Englewood Cliffs, NJ, 1965.
2. Rohrbach, C (Hrsg), "Handbuch für Experimentelle Spannungsanalyse", VDI-Verlag, Düsseldorf, 1989.
3. Ciba Specialty Chemicals, Performance Polymers Division, Duxford, Cambridge, CB2 4QA, UK.
4. Lambert, T H and Brailey, R J, Aeronautical Quarterly, 1962, 13, 17.
5. Stanley, P and Davies, M F, Österreichische Ingenieur und Architekten Zeitschrift, 1991, 136 Jahrgang, Heft 6, 275-284.
6. Timoshenko, S and Goodier, J N, "Theory of Elasticity", McGraw-Hill Book Company Inc, New York, 1951.
7. Bowden, F P and Tabor, D, "The Friction and Lubrication of Solids", Clarendon Press, Oxford, 1986.

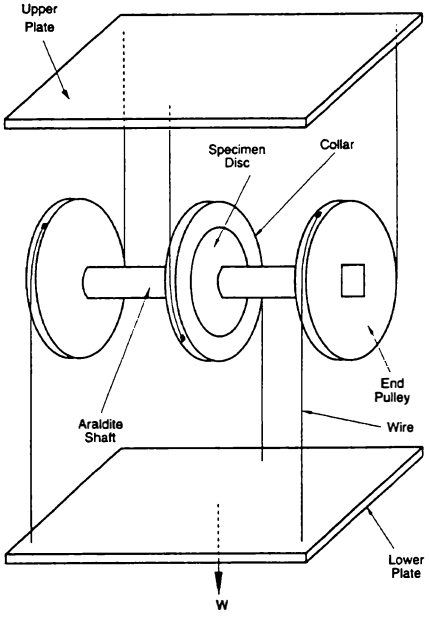

Fig.1 Test apparatus

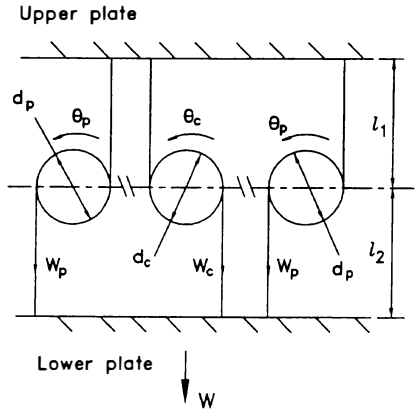

Fig.2 Forces and displacements

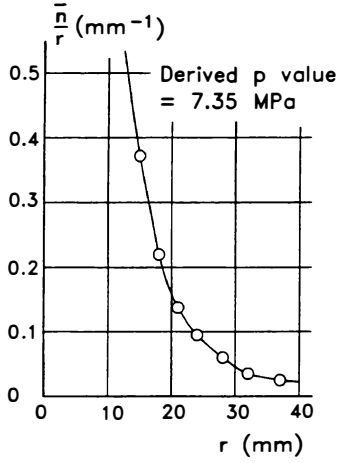

Fig.3 $(\bar{n}/r)$ versus r for 0.10mm interference

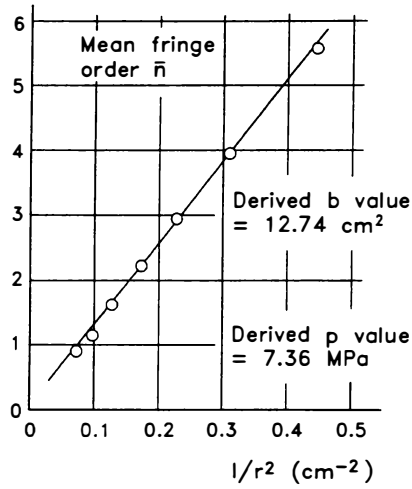

Fig.4 $\bar{n}$ versus $(1/r^2)$ for 0.10mm interference

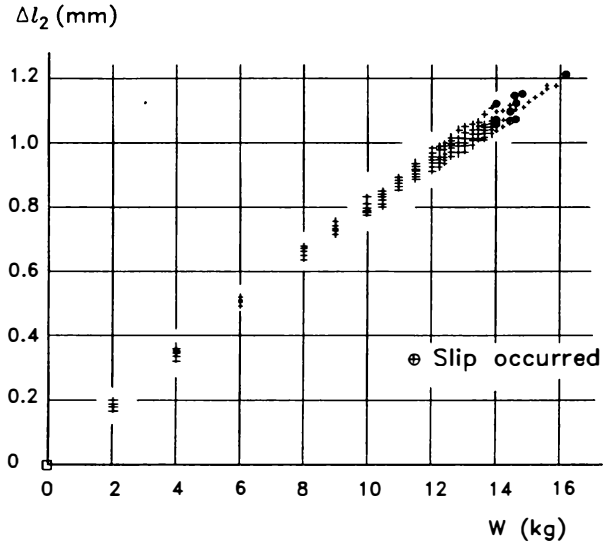

Fig.5 Typical load–displacement plots

Professor Peter Stanley,
School of Engineering, University of Manchester,
Oxford Road, Manchester M13 9PL, UK.
Tel. 0161 275 4303 Fax. 0161 275 4346